# *SUPPORTING INFORMATION FOR*

# From the design to the *in vivo* evaluation of benzohomoadamantane-derived soluble epoxide hydrolase inhibitors for the treatment of acute pancreatitis

*Sandra Codony[1], Carla Calvó-Tusell[2], Elena Valverde[1], Sílvia Osuna[2,3], Christophe* Morisseau[4], *M. Isabel Loza[5], José Brea[5], Concepción Pérez[6], María Isabel Rodríguez-Franco[6],* Javier *Pizarro-Delgado[7,8,9], Rubén Corpas[10,11], Christian Griñán-Ferré[12], Mercè Pallàs[12], Coral Sanfeliu[10,11], Manuel Vázquez-Carrera[7,8,9], Bruce D. Hammock[4], Ferran Feixas[2], Santiago Vázquez[1*]*

[1]Laboratori de Química Farmacèutica (Unitat Associada al CSIC), Departament de Farmacologia, Toxicologia i Química Terapèutica, Facultat de Farmàcia i Ciències de l'Alimentació, and Institute of Biomedicine (IBUB), Universitat de Barcelona, Av. Joan XXIII, 27-31, 08028 Barcelona, Spain.

[2]CompBioLab Group, Departament de Química and Institut de Química Computacional i Catàlisi (IQCC), Universitat de Girona, C/ Maria Aurèlia Capmany 69, 17003 Girona, Spain.

[3]Institució Catalana de Recerca i Estudis Avançats (ICREA), 08010 Barcelona, Spain.

[4]Department of Entomology and Nematology and Comprehensive Cancer Center, University of California, Davis, CA 95616, USA.

[5]Drug Screening Platform/Biofarma Research Group, CIMUS Research Center. Departamento de Farmacoloxía, Farmacia e Tecnoloxía Farmacéutica. University of Santiago de Compostela (USC), 15782 Santiago de Compostela, Spain.

[6]Institute of Medicinal Chemistry, Spanish National Research Council (CSIC), C/Juan de la Cierva 3, 28006 Madrid, Spain.

[7]Pharmacology Section. Department of Pharmacology, Toxicology and Medicinal Chemistry, Faculty of Pharmacy and Food Sciences, University of Barcelona, and Institute of Biomedicine of the University of Barcelona (IBUB), Av. Joan XXIII, 27-31, 08028 Barcelona, Spain.

[8]Spanish Biomedical Research Center in Diabetes and Associated Metabolic Diseases (CIBERDEM)-Instituto de Salud Carlos III, 28029 Madrid, Spain.

[9]Pediatric Research Institute-Hospital Sant Joan de Déu, 08950 Esplugues de Llobregat, Spain.

[10]Institute of Biomedical Research of Barcelona (IIBB), CSIC and IDIBAPS, 08036 Barcelona, Spain.

[11]CIBER Epidemiology and Public Health (CIBERESP)-Instituto de Salud Carlos III, 28029, Madrid, Spain.

[12]Pharmacology Section. Department of Pharmacology, Toxicology and Medicinal Chemistry, Faculty of Pharmacy and Food Sciences, and Institut de Neurociències, University of Barcelona, Av. Joan XXIII, 27-31, 08028 Barcelona, Spain.

* Corresponding author. Tel.: +34 934024533; *E-mail address:* svazquez@ub.edu *(S. Vázquez).*

# Table of contents

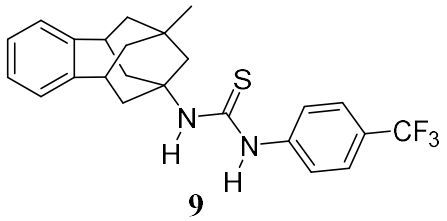
S
N
H
N
H
CF3

**9**

,

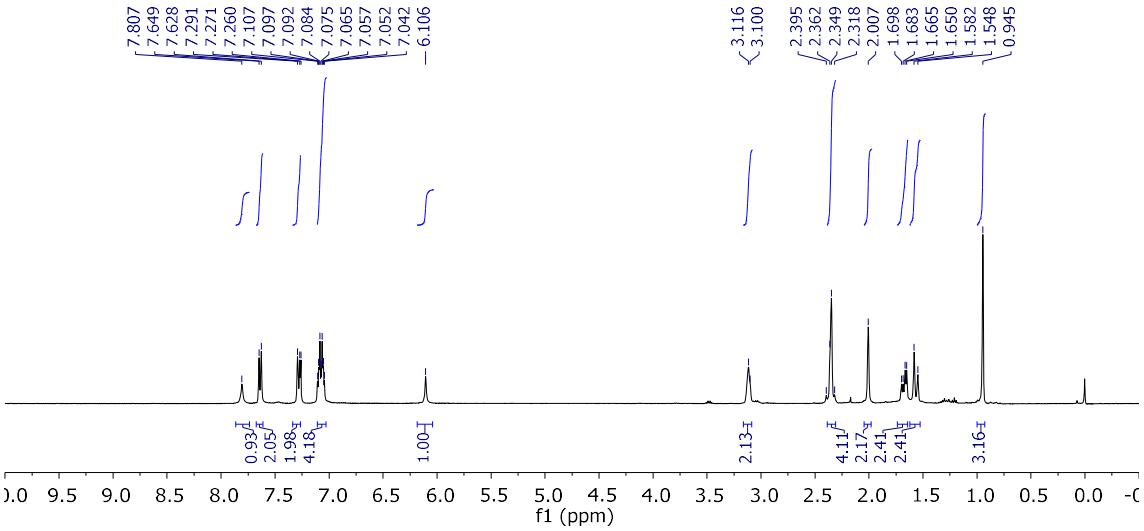
7.807
7.649
7.628
7.291
7.271
7.260
7.107
7.097
7.092
7.084
7.075
7.065
7.057
7.052
7.042
6.106
3.116
3.100
2.395
2.362
2.349
2.318
2.007
1.698
1.683
1.665
1.650
1.582
1.548
0.945
0.93
2.05
1.98
4.18
1.00
2.13
4.11
2.17
2.41
2.41
3.16
f1 (ppm)

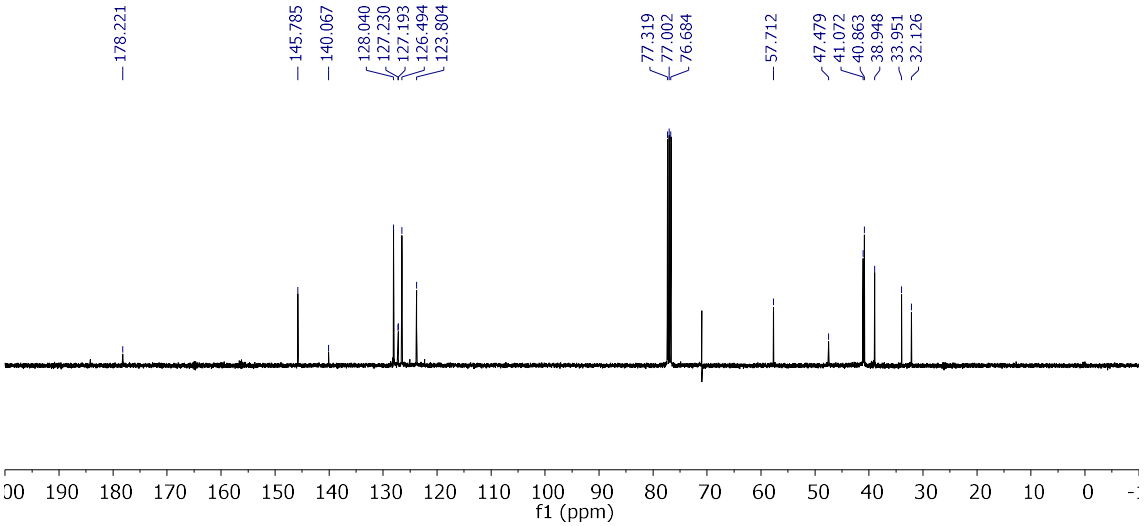
178.221
145.785
140.067
128.040
127.230
127.193
126.494
123.804
77.319
77.002
76.684
57.712
47.479
41.072
40.863
38.948
33.951
32.126
f1 (ppm)

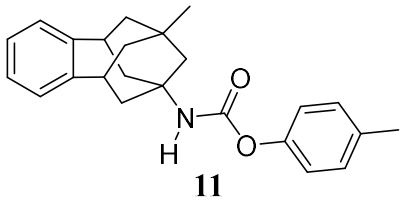
O
N
H
O

**11**

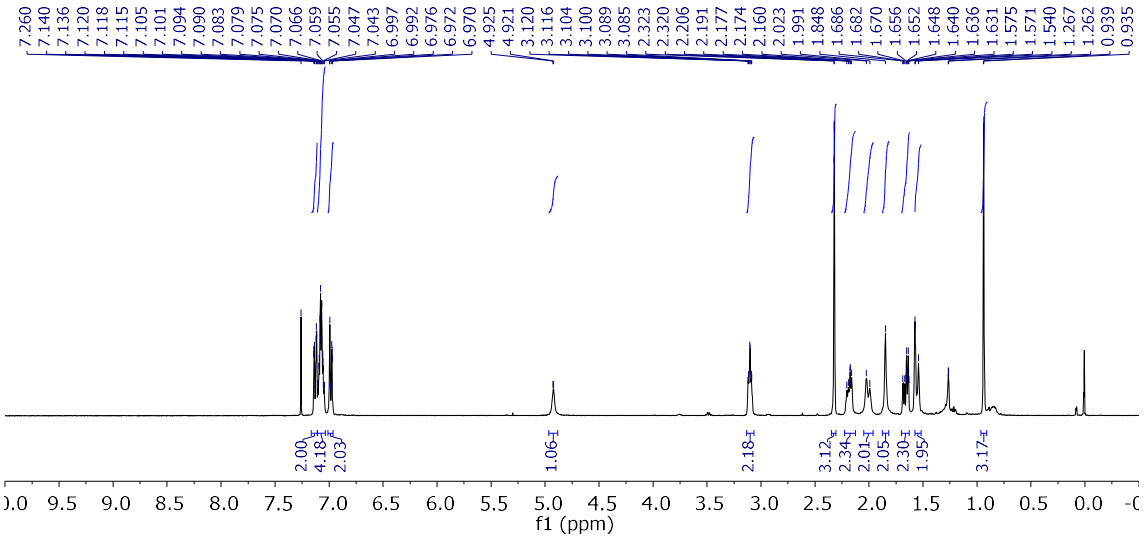
7.260
7.140
7.136
7.120
7.118
7.115
7.105
7.101
7.094
7.090
7.083
7.079
7.075
7.070
7.066
7.059
7.055
7.047
7.043
6.997
6.992
6.976
6.972
6.970
4.925
4.921
3.120
3.116
3.104
3.100
3.089
3.085
2.323
2.320
2.206
2.191
2.177
2.174
2.160
2.023
1.991
1.848
1.686
1.682
1.670
1.656
1.652
1.648
1.640
1.636
1.631
1.575
1.571
1.540
1.267
1.262
0.939
0.935
2.00
4.18
2.03
1.06
2.18
3.12
2.34
2.01
2.05
2.30
1.95
3.17
f1 (ppm)

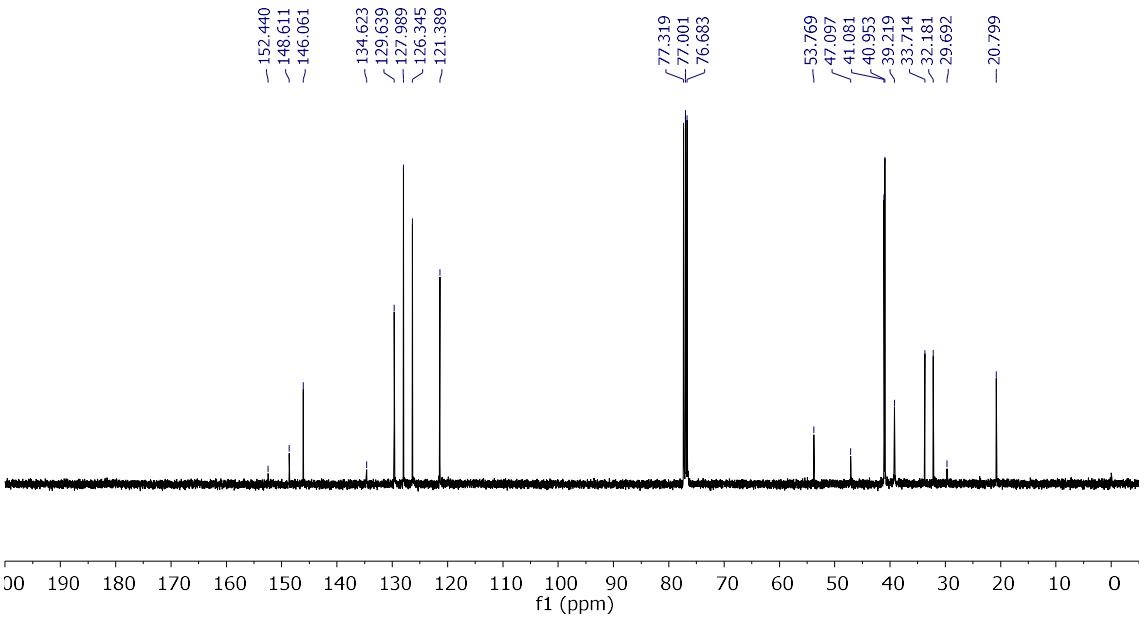
152.440
148.611
146.061
134.623
129.639
127.989
126.345
121.389
77.319
77.001
76.683
53.769
47.097
41.081
40.953
39.219
33.714
32.181
29.692
20.799
f1 (ppm)

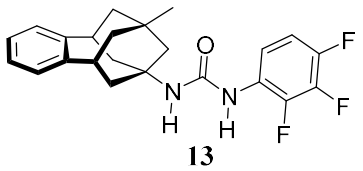
O
N
H
N
H
F
F
F

**13**

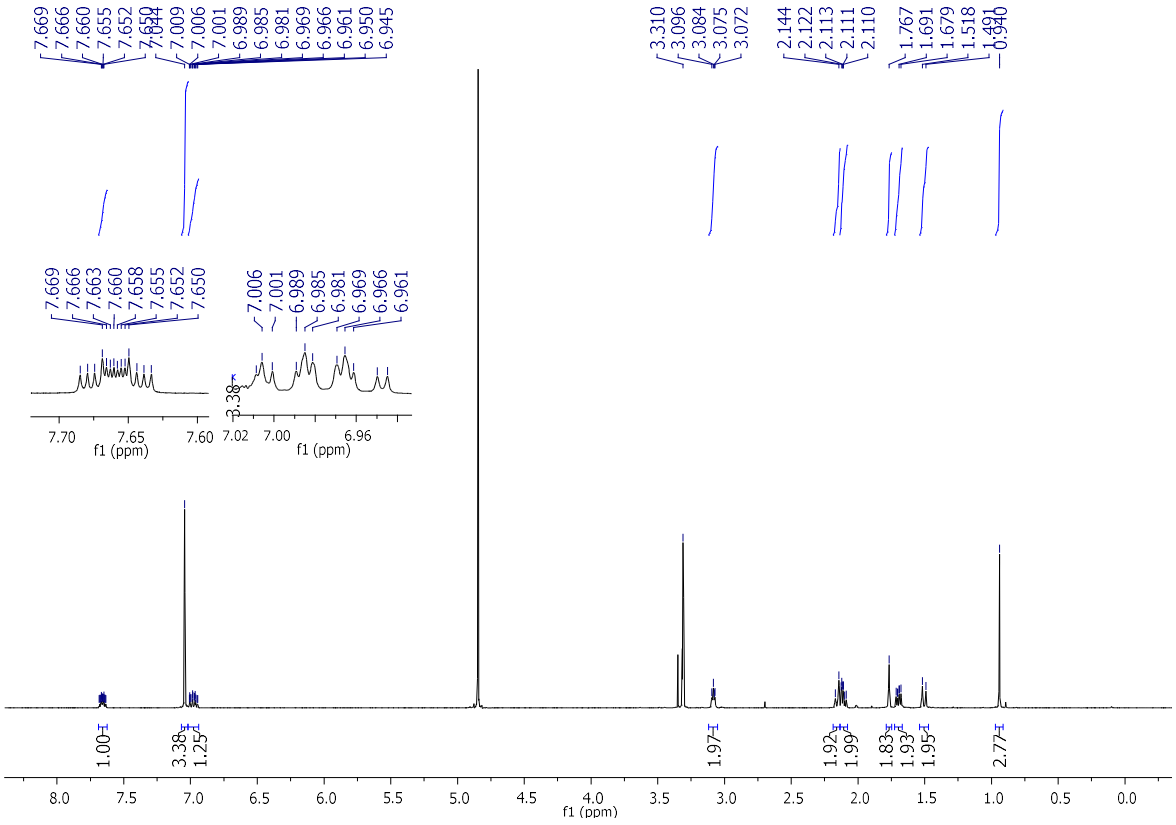
7.669
7.666
7.660
7.655
7.652
7.650
7.044
7.009
7.006
7.001
6.989
6.985
6.981
6.969
6.966
6.961
6.950
6.945
3.310
3.096
3.084
3.075
3.072
2.144
2.122
2.113
2.111
2.110
1.767
1.691
1.679
1.518
1.491
0.940
1.00
3.38
1.25
1.97
1.92
1.99
1.83
1.93
1.95
2.77
f1 (ppm)

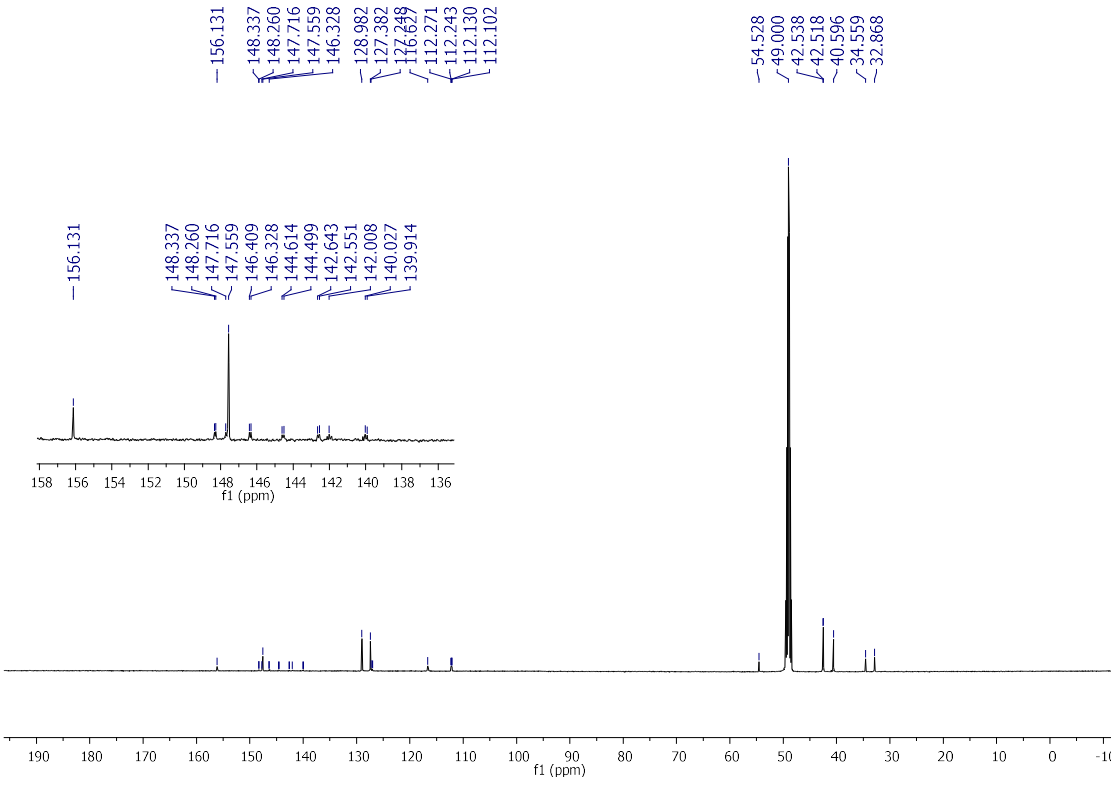
156.131
148.337
148.260
147.716
147.559
146.328
128.982
127.382
112.271
112.243
112.130
112.102
54.528
49.000
42.538
42.518
40.596
34.559
32.868
146.409
144.614
144.499
142.643
142.551
142.008
140.027
139.914
f1 (ppm)

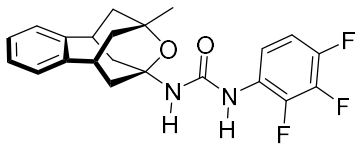
O
O
N
H
N
H
F
F
F

**14**

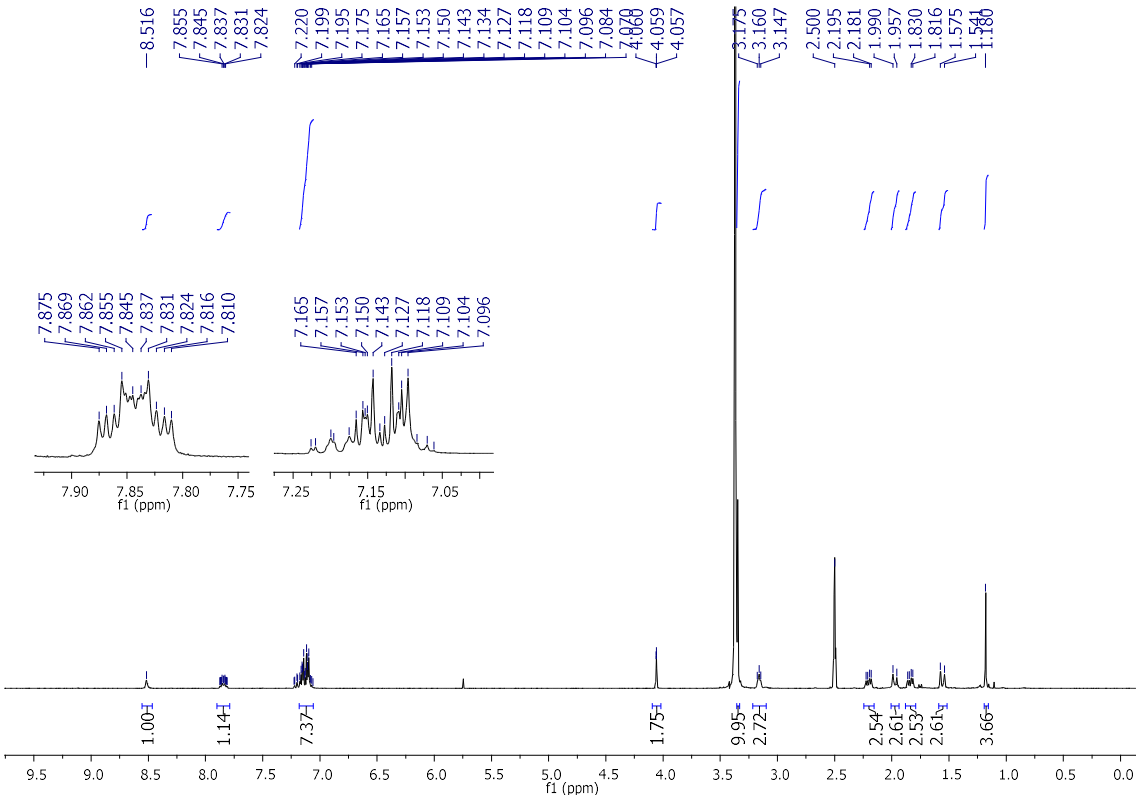
8.516
7.855
7.845
7.837
7.831
7.824
7.220
7.199
7.195
7.175
7.165
7.157
7.153
7.150
7.143
7.134
7.127
7.118
7.109
7.104
7.096
7.084
4.059
4.057
3.175
3.160
3.147
2.500
2.195
2.181
1.990
1.957
1.830
1.816
1.575
1.541
1.180
7.875
7.869
7.862
7.855
7.845
7.837
7.831
7.824
7.816
7.810
7.165
7.157
7.153
7.150
7.143
7.127
7.118
7.109
7.104
7.096
f1 (ppm)
1.00
1.14
7.37
1.75
9.95
2.72
2.54
2.61
2.53
2.61
3.66
f1 (ppm)

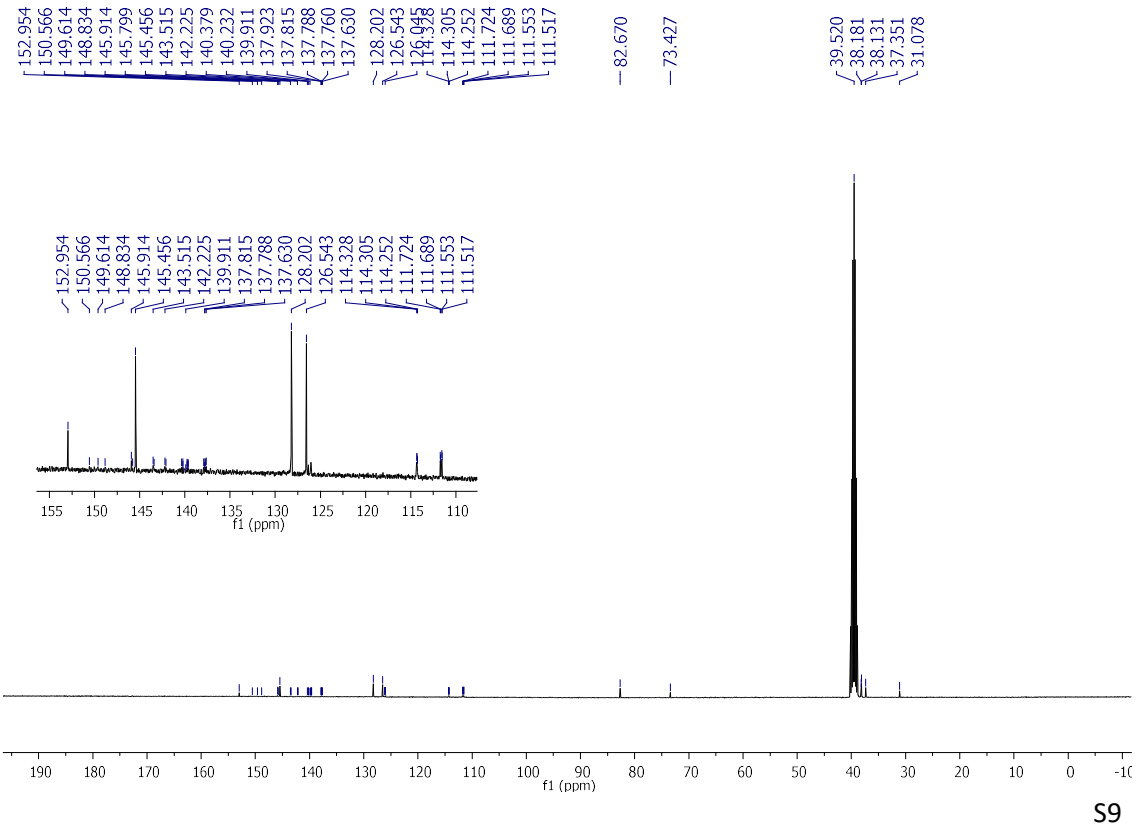
152.954
150.566
149.614
148.834
145.914
145.799
145.456
143.515
142.225
140.379
140.232
139.911
137.923
137.815
137.788
137.760
137.630
128.202
126.543
126.045
114.328
114.305
114.252
111.724
111.689
111.553
111.517
82.670
73.427
39.520
38.181
38.131
37.351
31.078
f1 (ppm)

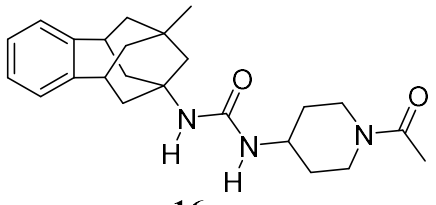

**16**

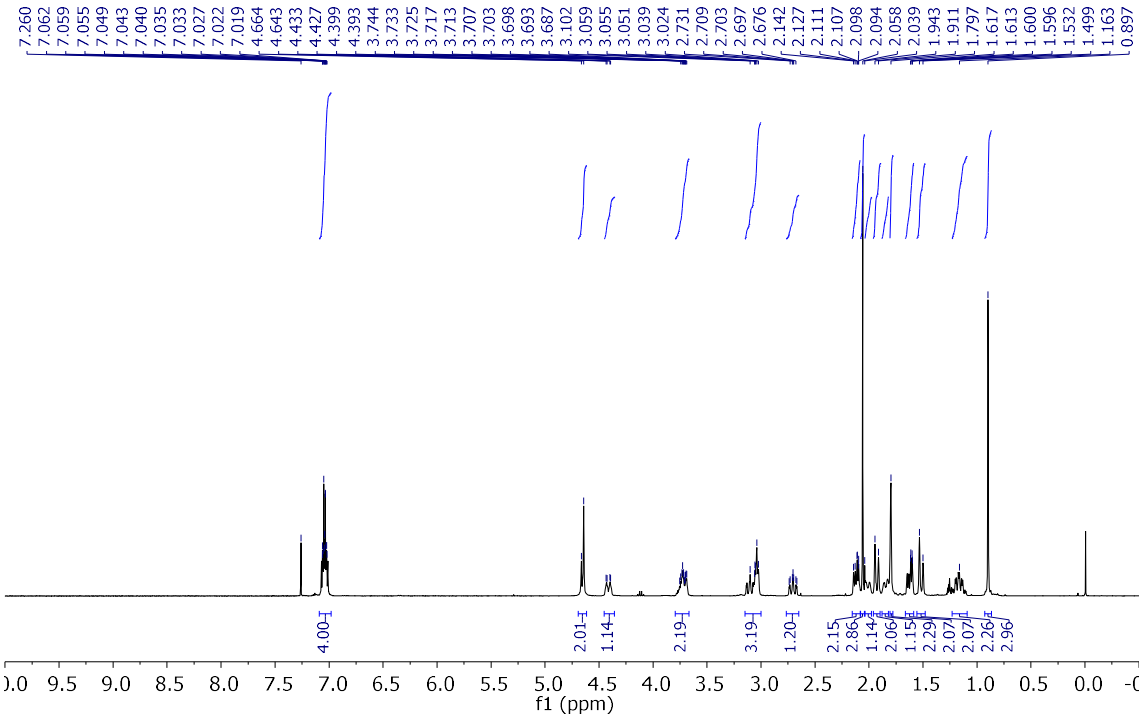
7.260
7.062
7.059
7.055
7.049
7.043
7.040
7.035
7.033
7.027
7.022
7.019
4.664
4.643
4.433
4.427
4.399
4.393
3.744
3.733
3.725
3.717
3.713
3.707
3.703
3.698
3.693
3.687
3.102
3.059
3.055
3.051
3.039
3.024
2.731
2.709
2.703
2.697
2.676
2.142
2.127
2.111
2.107
2.098
2.094
2.058
2.039
1.943
1.911
1.797
1.617
1.613
1.600
1.596
1.532
1.499
1.163
0.897
4.00
2.01
1.14
2.19
3.19
1.20
2.15
2.86
1.14
2.06
1.15
2.29
2.07
2.07
2.26
2.96
f1 (ppm)

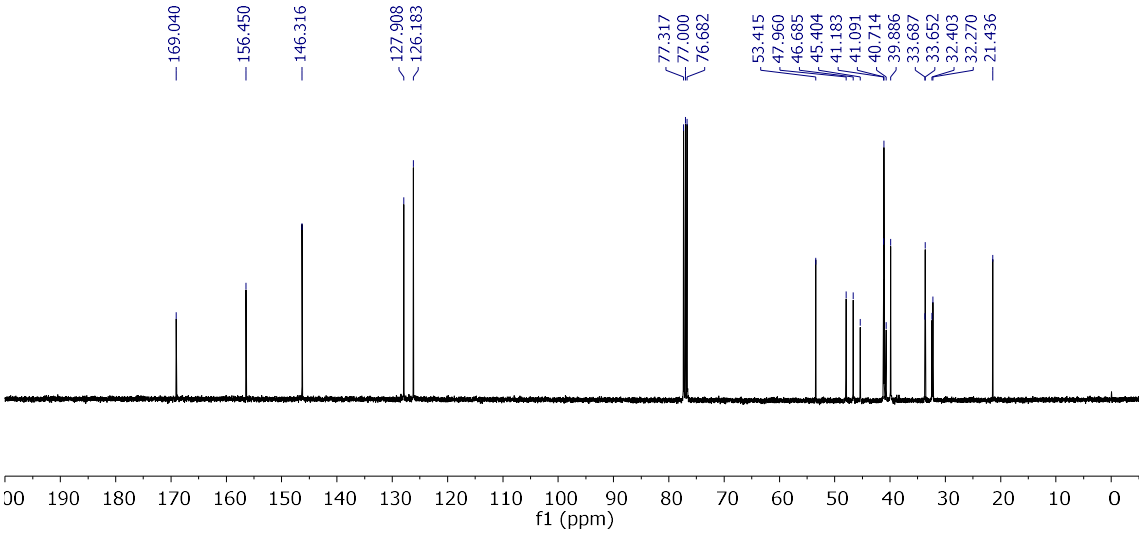
169.040
156.450
146.316
127.908
126.183
77.317
77.000
76.682
53.415
47.960
46.685
45.404
41.183
41.091
40.714
39.886
33.687
33.652
32.403
32.270
21.436
f1 (ppm)

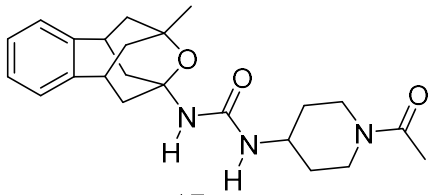

**17**

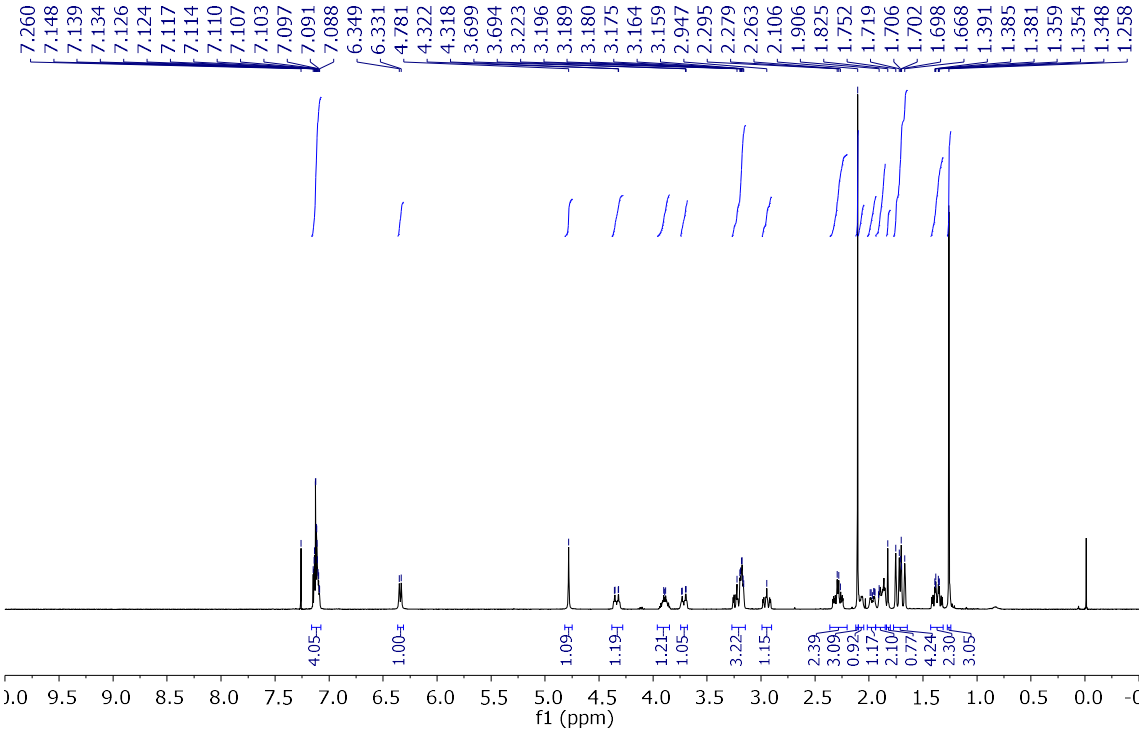
7.260
7.148
7.139
7.134
7.126
7.124
7.117
7.114
7.110
7.107
7.103
7.097
7.091
7.088
6.349
6.331
4.781
4.322
4.318
3.699
3.694
3.223
3.196
3.189
3.180
3.175
3.164
3.159
2.947
2.295
2.279
2.263
2.106
1.906
1.825
1.752
1.719
1.706
1.702
1.698
1.668
1.391
1.385
1.381
1.359
1.354
1.348
1.258
4.05
1.00
1.09
1.19
1.21
1.05
3.22
1.15
2.39
3.09
0.92
1.17
2.10
0.77
4.24
2.30
3.05
f1 (ppm)

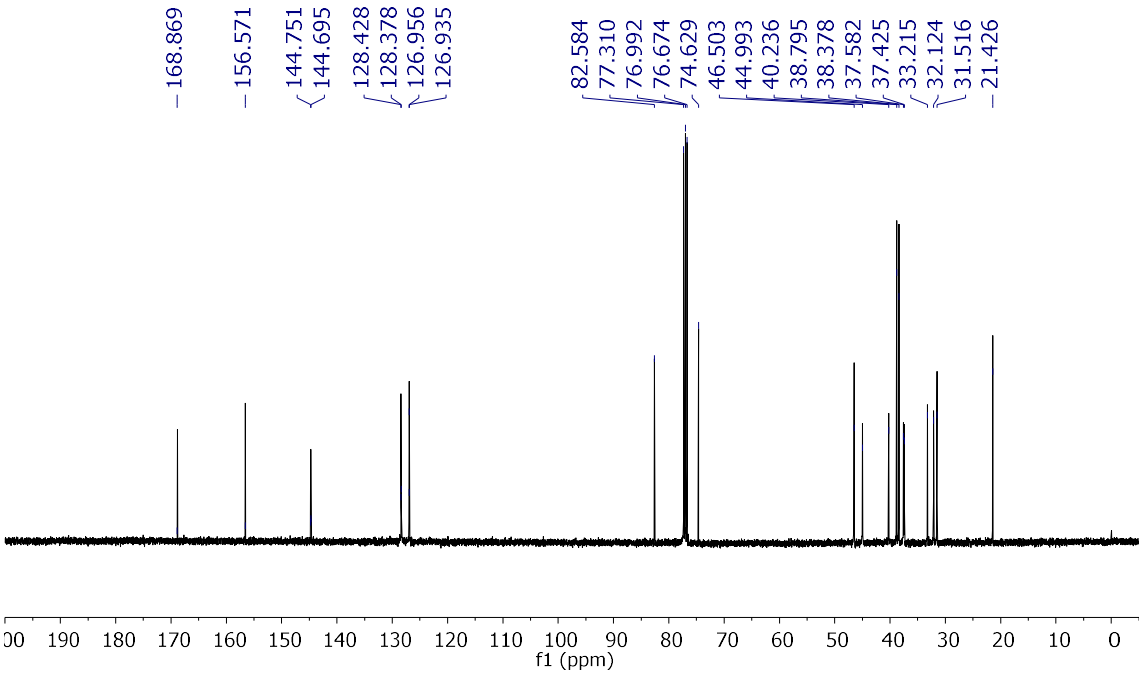
168.869
156.571
144.751
144.695
128.428
128.378
126.956
126.935
82.584
77.310
76.992
76.674
74.629
46.503
44.993
40.236
38.795
38.378
37.582
37.425
33.215
32.124
31.516
21.426
f1 (ppm)

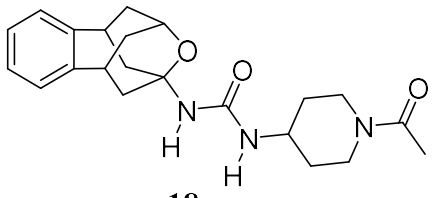

**18**

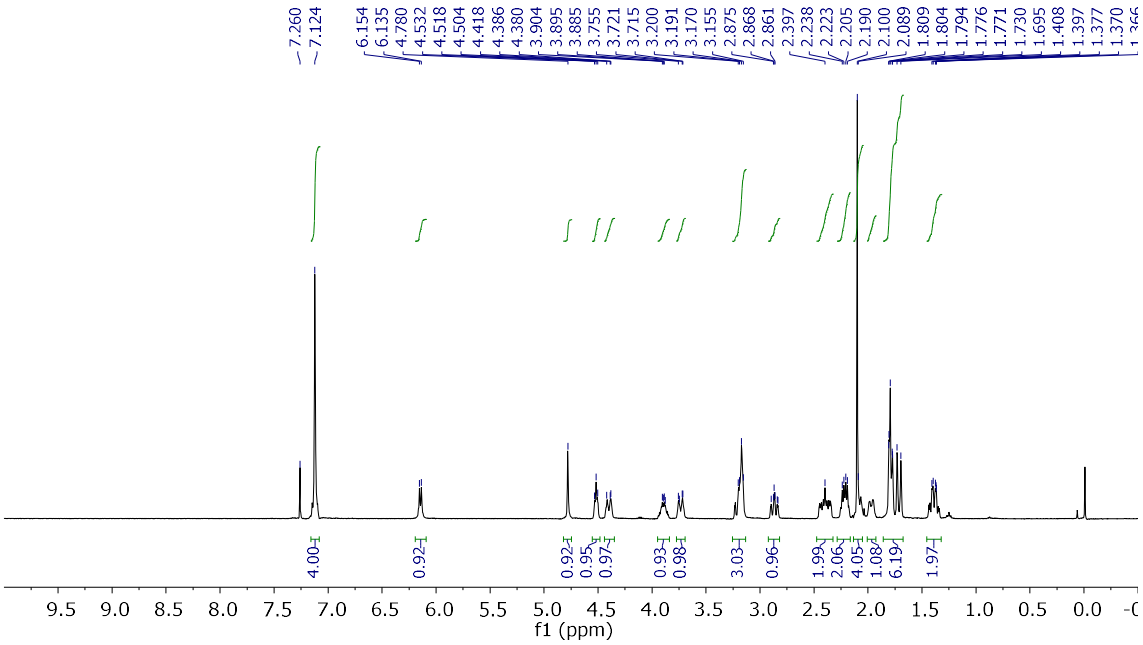
7.260
7.124
6.154
6.135
4.780
4.532
4.518
4.504
4.418
4.386
4.380
3.904
3.895
3.885
3.755
3.721
3.715
3.200
3.191
3.170
3.155
2.875
2.868
2.861
2.397
2.238
2.223
2.205
2.190
2.100
2.089
1.809
1.804
1.794
1.776
1.771
1.730
1.695
1.408
1.397
1.377
1.370
4.00
0.92
0.92
0.95
0.97
0.93
0.98
3.03
0.96
1.99
2.06
4.05
1.08
6.19
1.97
f1 (ppm)

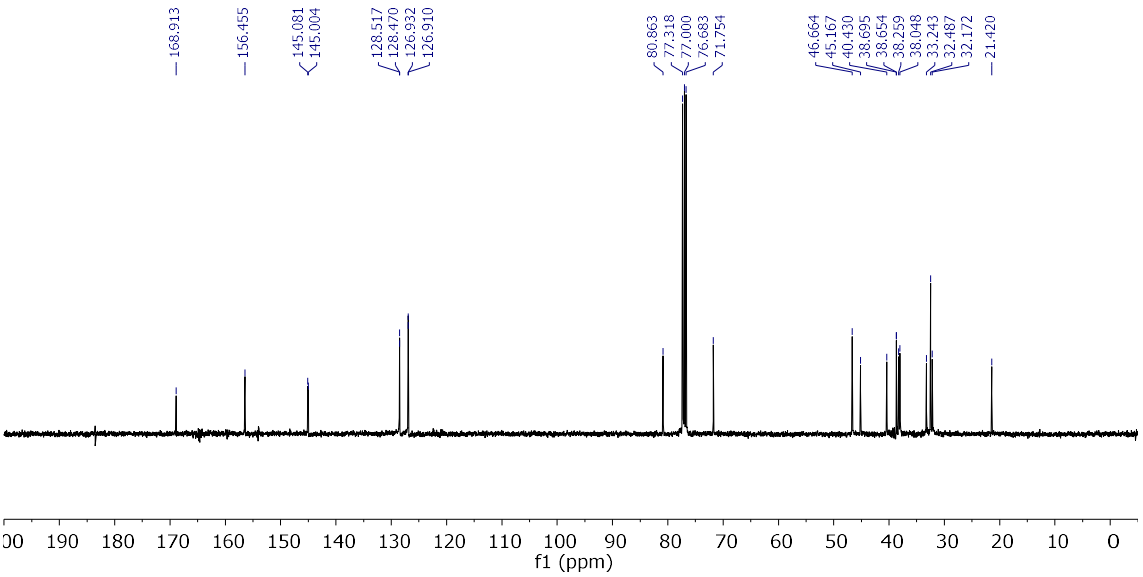
168.913
156.455
145.081
145.004
128.517
128.470
126.932
126.910
80.863
77.318
77.000
76.683
71.754
46.664
45.167
40.430
38.695
38.654
38.259
38.048
33.243
32.487
32.172
21.420
f1 (ppm)

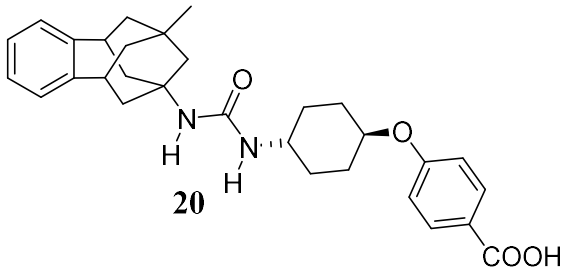
O
N
H
N
H
O
COOH

**20**

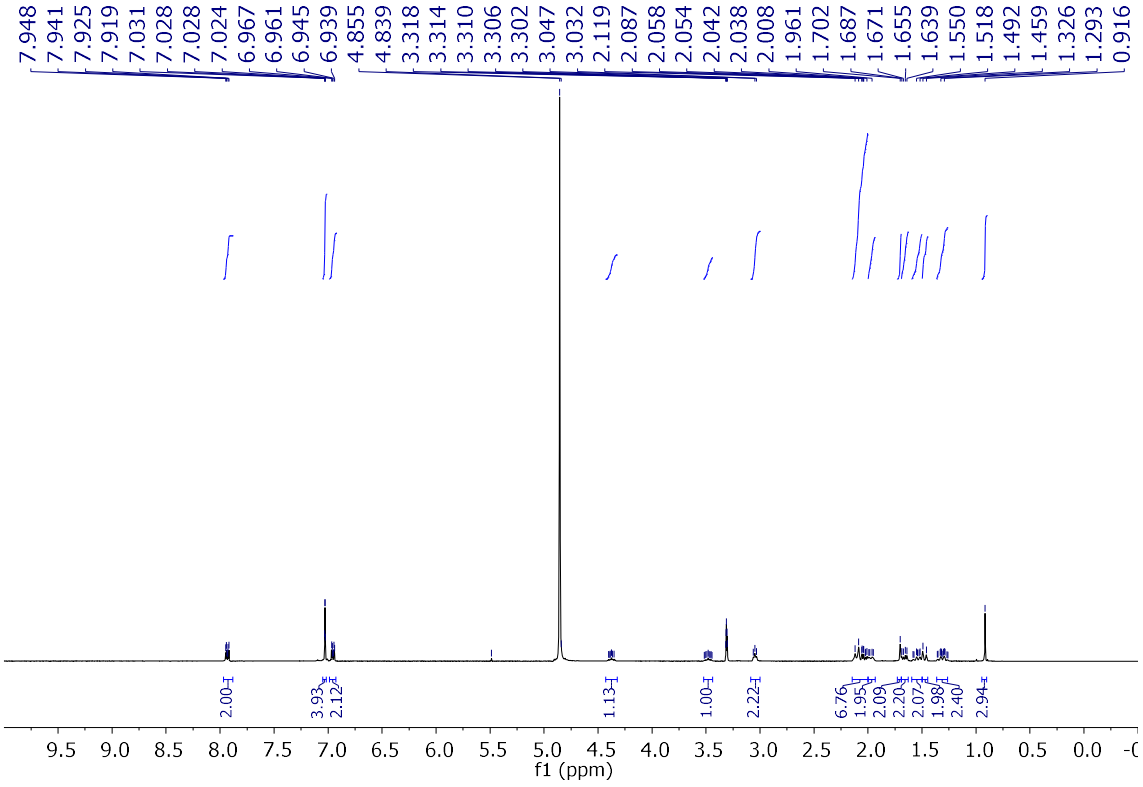
7.948
7.941
7.925
7.919
7.031
7.028
7.028
7.024
6.967
6.961
6.945
6.939
4.855
4.839
3.318
3.314
3.310
3.306
3.302
3.047
3.032
2.119
2.087
2.058
2.054
2.042
2.038
2.008
1.961
1.702
1.687
1.671
1.655
1.639
1.550
1.518
1.492
1.459
1.326
1.293
0.916
2.00
3.93
2.12
1.13
1.00
2.22
6.76
1.95
2.09
2.20
2.07
1.98
2.40
2.94
9.5 9.0 8.5 8.0 7.5 7.0 6.5 6.0 5.5 5.0 4.5 4.0 3.5 3.0 2.5 2.0 1.5 1.0 0.5 0.0
f1 (ppm)

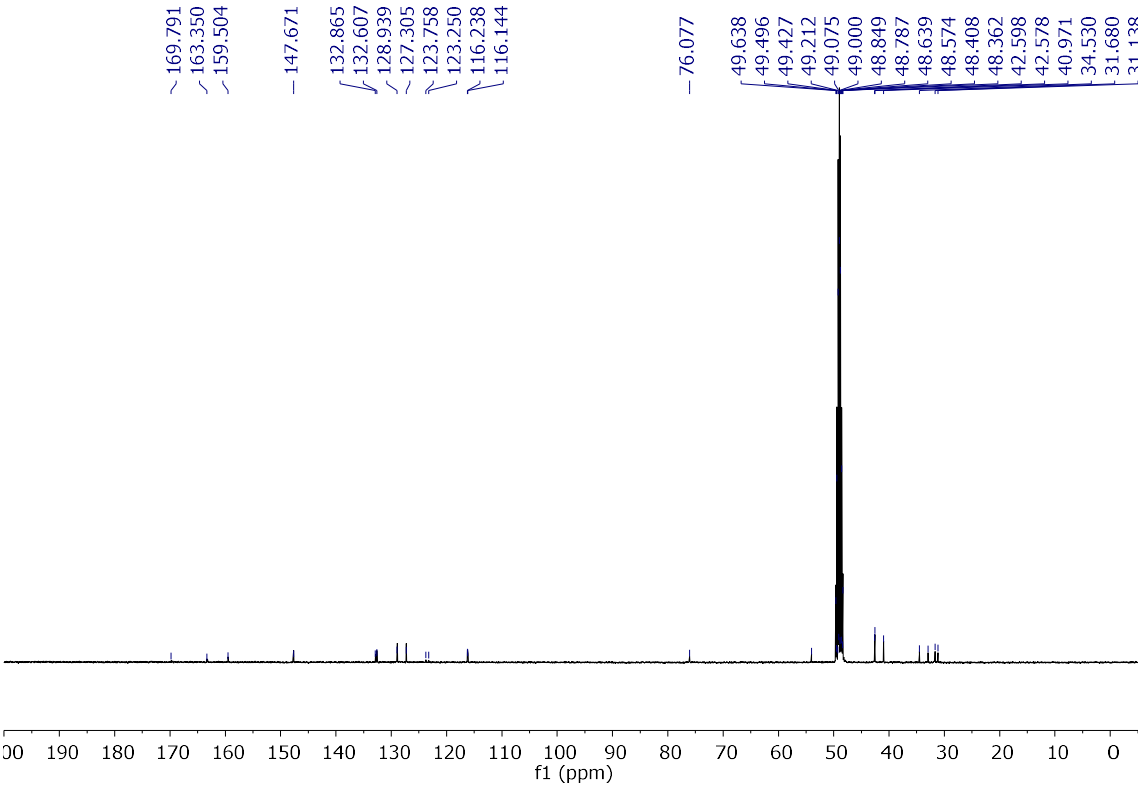
169.791
163.350
159.504
147.671
132.865
132.607
128.939
127.305
123.758
123.250
116.238
116.144
76.077
49.638
49.496
49.427
49.212
49.075
49.000
48.849
48.787
48.639
48.574
48.408
48.362
42.598
42.578
40.971
34.530
31.680
190 180 170 160 150 140 130 120 110 100 90 80 70 60 50 40 30 20 10 0
f1 (ppm)

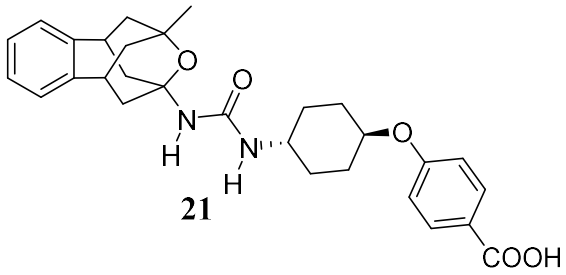
O
O
N
H
N
H
O
COOH

**21**

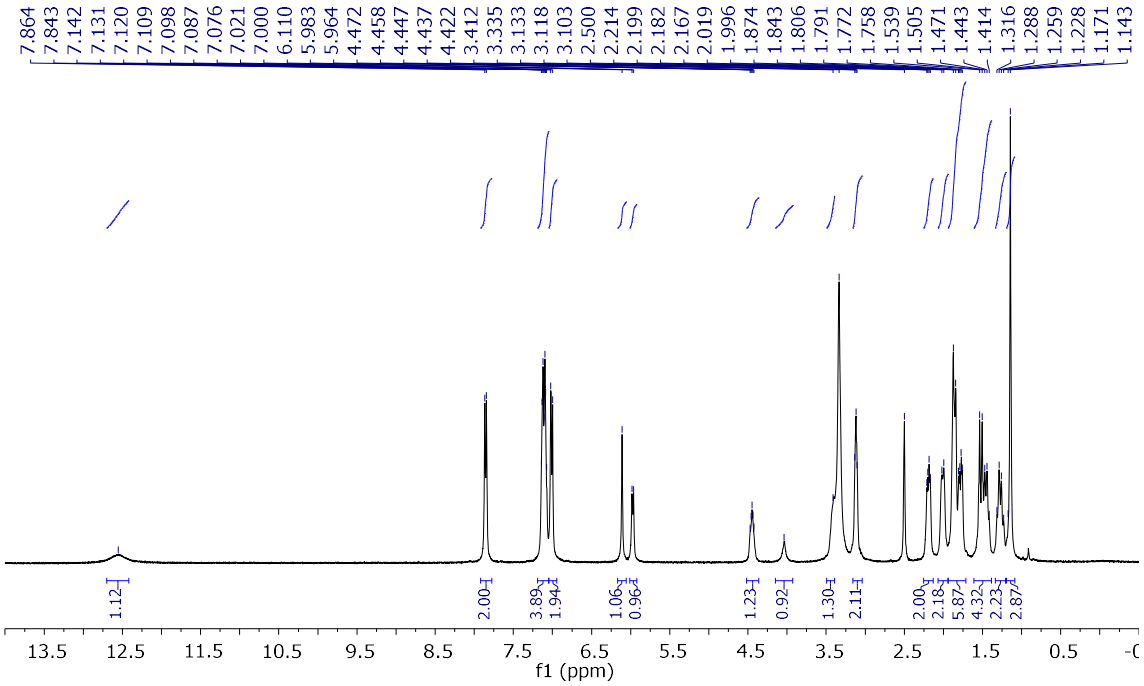
7.864
7.843
7.142
7.131
7.120
7.109
7.098
7.087
7.076
7.021
7.000
6.110
5.983
5.964
4.472
4.458
4.447
4.437
4.422
3.412
3.335
3.133
3.118
3.103
2.500
2.214
2.199
2.182
2.167
2.019
1.996
1.874
1.843
1.806
1.791
1.772
1.758
1.539
1.505
1.471
1.443
1.414
1.316
1.288
1.259
1.228
1.171
1.143
1.12
2.00
3.89
1.94
1.06
0.96
1.23
0.92
1.30
2.11
2.00
2.18
5.87
4.32
2.23
2.87
13.5
12.5
11.5
10.5
9.5
8.5
7.5
6.5
5.5
4.5
3.5
2.5
1.5
0.5
f1 (ppm)

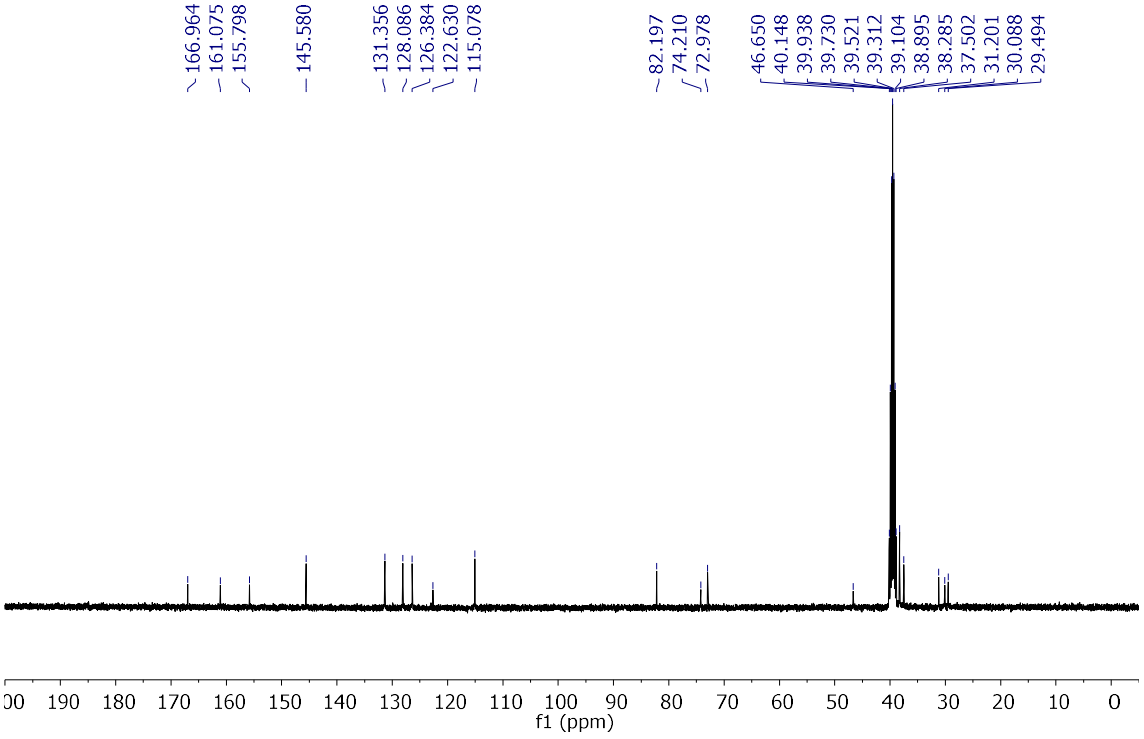
166.964
161.075
155.798
145.580
131.356
128.086
126.384
122.630
115.078
82.197
74.210
72.978
46.650
40.148
39.938
39.730
39.521
39.312
39.104
38.895
38.285
37.502
31.201
30.088
29.494
190
180
170
160
150
140
130
120
110
100
90
80
70
60
50
40
30
20
10
0
f1 (ppm)

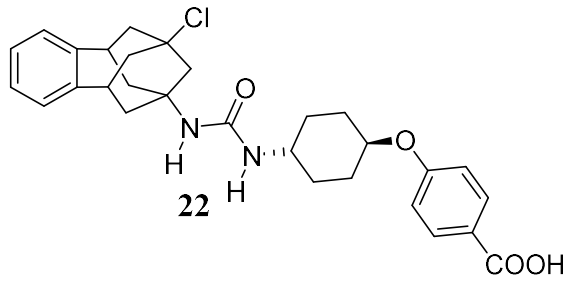
Cl
O
N
H
N
H
O
COOH

**22**

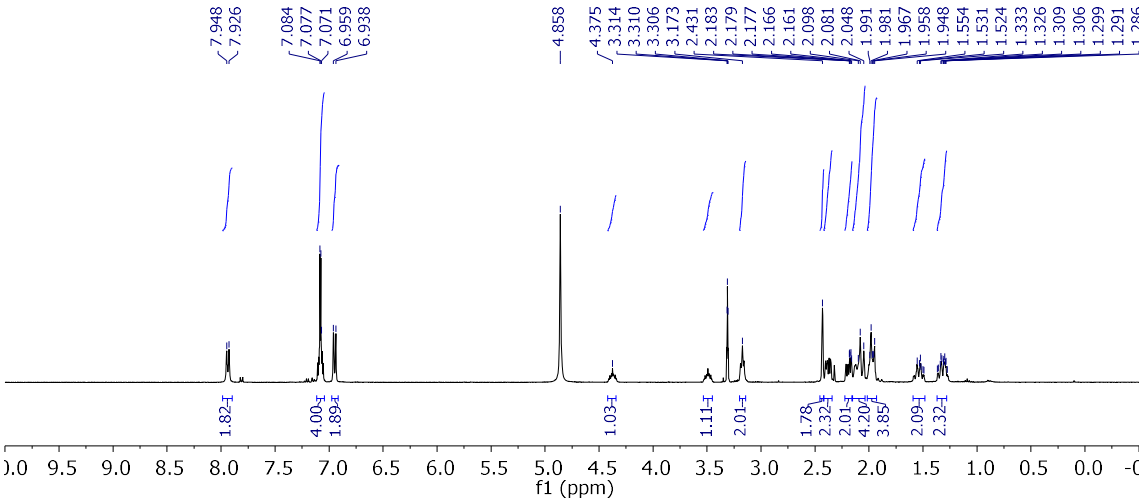
7.948
7.926
7.084
7.077
7.071
6.959
6.938
4.858
4.375
3.314
3.310
3.306
3.173
2.431
2.183
2.179
2.177
2.166
2.161
2.098
2.081
2.048
1.991
1.981
1.967
1.958
1.948
1.554
1.531
1.524
1.333
1.326
1.309
1.306
1.299
1.291
1.82
4.00
1.89
1.03
1.11
2.01
1.78
2.32
2.01
4.20
3.85
2.09
2.32
f1 (ppm)

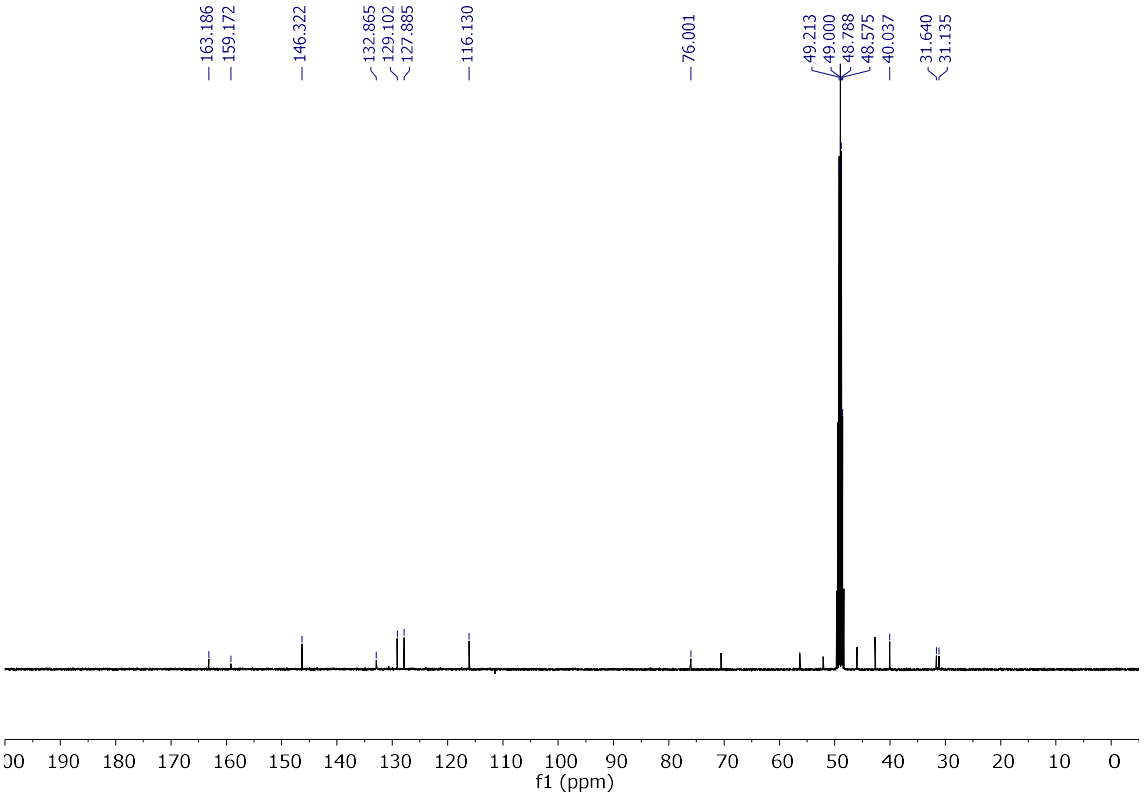
163.186
159.172
146.322
132.865
129.102
127.885
116.130
76.001
49.213
49.000
48.788
48.575
40.037
31.640
31.135
f1 (ppm)

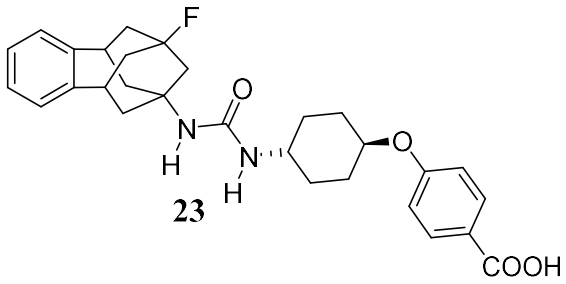
F
O
N
H
N
H
O
COOH

**23**

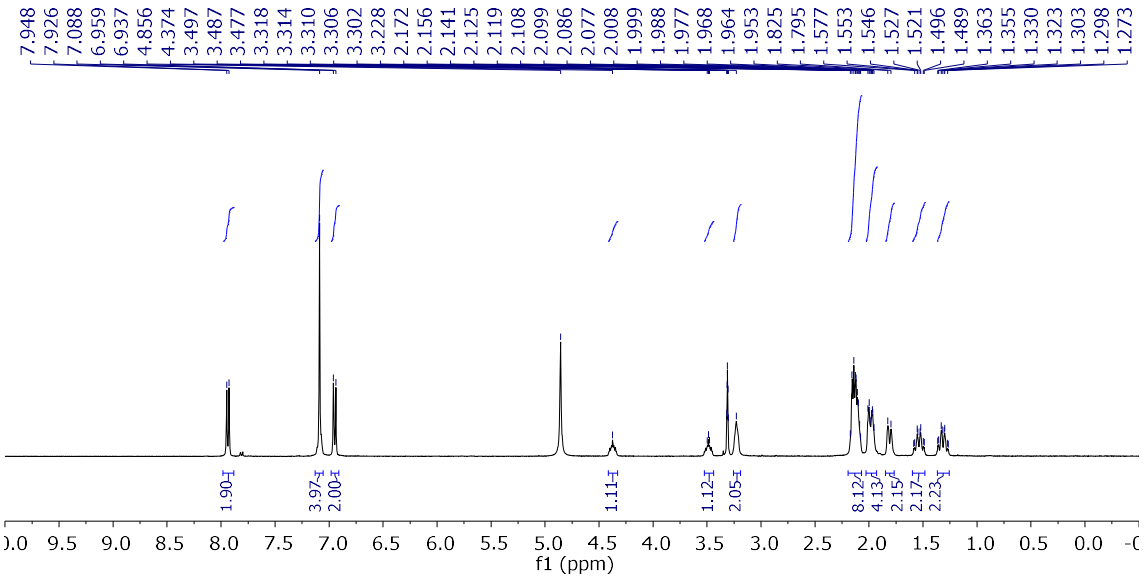
7.948
7.926
7.088
6.959
6.937
4.856
4.374
3.497
3.487
3.477
3.318
3.314
3.310
3.306
3.302
3.228
2.172
2.156
2.141
2.125
2.119
2.108
2.099
2.086
2.077
2.008
1.999
1.988
1.977
1.968
1.964
1.953
1.825
1.795
1.577
1.553
1.546
1.527
1.521
1.496
1.489
1.363
1.355
1.330
1.323
1.303
1.298
1.273
1.90
3.97
2.00
1.11
1.12
2.05
8.12
4.13
2.15
2.17
2.23
f1 (ppm)

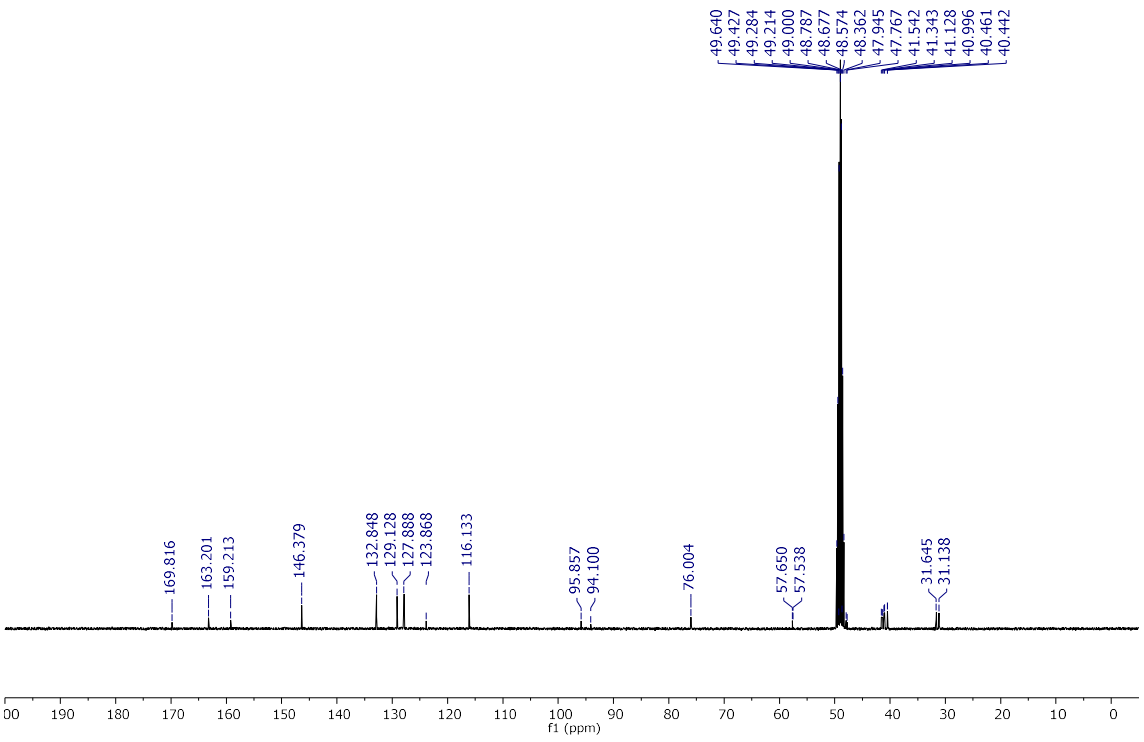
49.640
49.427
49.284
49.214
49.000
48.787
48.677
48.574
48.362
47.945
47.767
41.542
41.343
41.128
40.996
40.461
40.442
169.816
163.201
159.213
146.379
132.848
129.128
127.888
123.868
116.133
95.857
94.100
76.004
57.650
57.538
31.645
31.138
f1 (ppm)

| Compound | Molecular Formula | Calculated | | | Found | | |
|---|---|---|---|---|---|---|---|
| | | C | H | N | C | H | N |
| **9** | $C_{24}H_{25}F_3N_2S$ | 66.96 | 5.85 | 6.51 | 66.79 | 5.95 | 6.37 |
| **11** | $C_{24}H_{27}NO_2 \cdot 0.15\ H_2O$ | 79.15 | 7.56 | 3.85 | 79.34 | 7.92 | 3.48 |
| **13** | $C_{23}H_{23}F_3N_2O$ | 68.99 | 5.79 | 7.00 | 68.94 | 5.92 | 6.71 |
| **14** | $C_{22}H_{21}F_3N_2O_2 \cdot 0.1\ H_2O$ | 65.37 | 5.29 | 6.93 | 65.18 | 5.31 | 6.73 |
| **16** | $C_{24}H_{33}N_3O_2 \cdot 0.25$ EtOAc | 71.91 | 8.45 | 10.06 | 71.73 | 8.43 | 10.27 |
| **17** | $C_{23}H_{31}N_3O_3$ | 69.49 | 7.86 | 10.57 | 69.47 | 7.92 | 10.38 |
| **18** | $C_{22}H_{29}N_3O_3 \cdot 0.95\ H_2O$ | 65.96 | 7.77 | 10.49 | 66.25 | 7.67 | 10.13 |
| **20** | $C_{30}H_{36}N_2O_4 \cdot 1.5\ H_2O$ | 69.88 | 7.62 | 5.43 | 69.53 | 7.37 | 5.10 |
| **21** | $C_{29}H_{34}N_2O_5 \cdot 0.5\ CH_2Cl_2$ | 66.06 | 6.58 | 5.21 | 66.20 | 6.43 | 5.17 |
| **22** | $C_{29}H_{33}ClN_2O_4 \cdot 1\ CH_3OH$ | 66.59 | 6.89 | 5.18 | 66.85 | 6.62 | 4.91 |
| **23** | $C_{29}H_{33}FN_2O_4 \cdot 0.45\ CH_3OH$ | 69.77 | 6.92 | 5.53 | 69.68 | 6.79 | 5.57 |

**Table S1**: Elemental analysis data.

HPLC trace for compound **22**

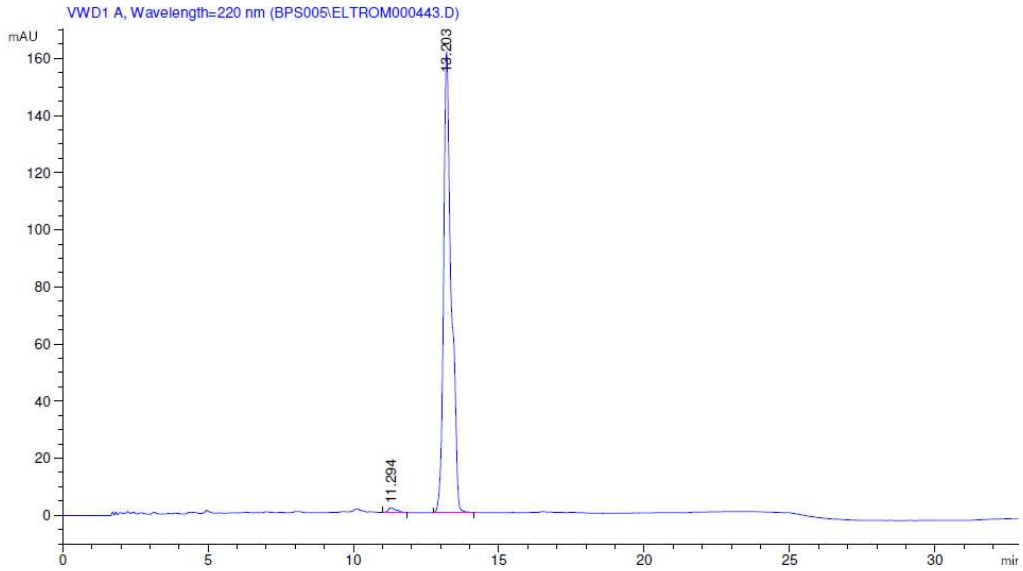


Signal 1: VWD1 A, Wavelength=220 nm

| Peak # | RetTime [min] | Type | Width [min] | Area mAU *s | Height [mAU ] | Area % |
|---|---|---|---|---|---|---|
| 1 | 11.294 | BB | 0.2786 | 33.87679 | 1.70337 | 1.1300 |
| 2 | 13.203 | BB | 0.2636 | 2964.20068 | 161.49048 | 98.8700 |
| Totals : | | | | 2998.07747 | 163.19384 | |

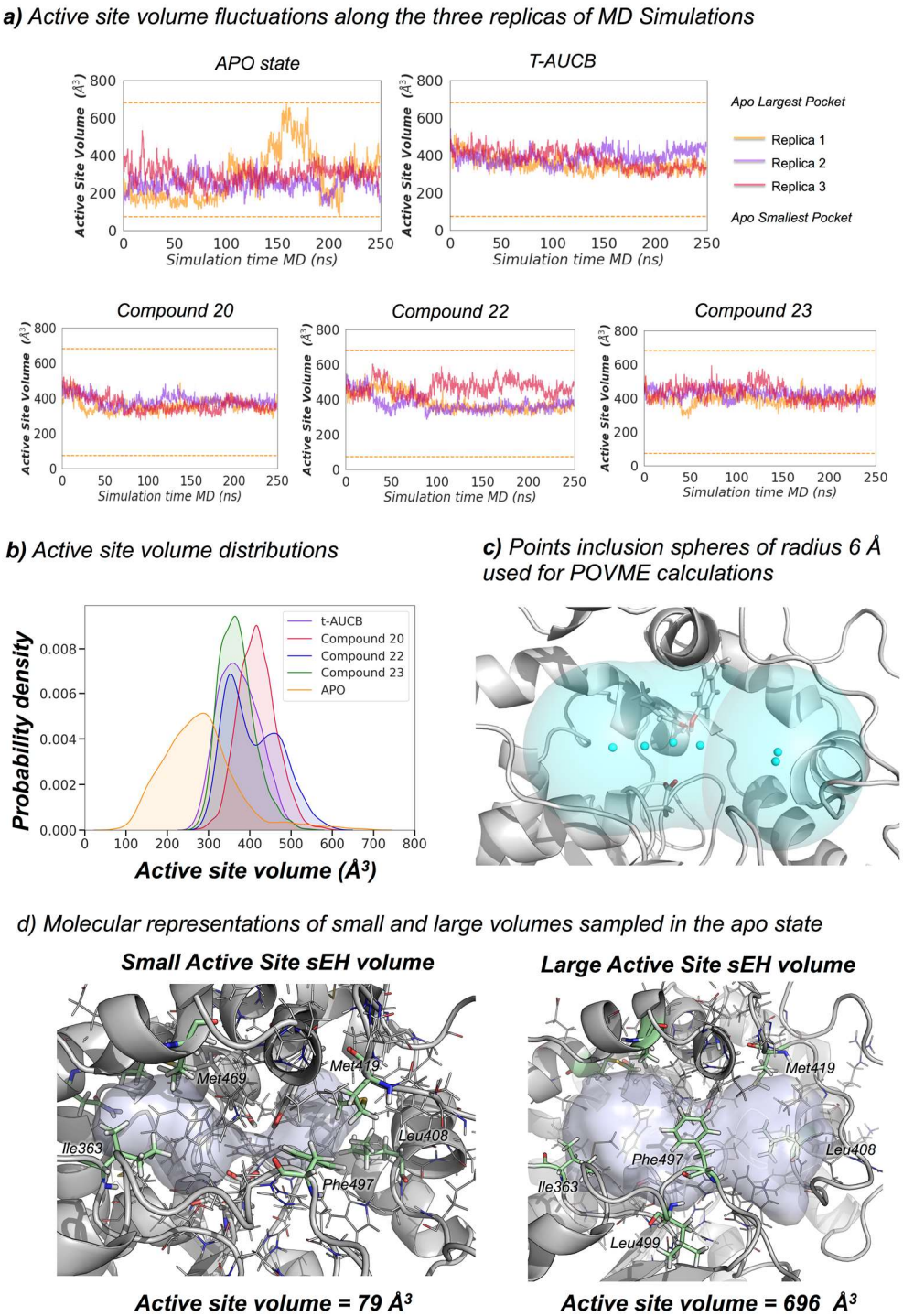


**Figure S1**: a) Representation of the active site volume fluctuations in the different MD replicas and systems considered calculated using the using the POcket Volume Measurer.[1] b) Probability density of the active site volumes for the apo state simulations (orange), and inhibitor bound simulations: *t*-AUCB (purple), **20** (red), **22** (blue), and **23** (green). c) Visualization of the 6 Å inclusion spheres used for POVME active site volume calculations. d) Representative MD snapshots displaying either small (left panel) or large active site sEH volumes (right panel) are shown. The most important residues affecting the volume are shown in sticks and labelled.

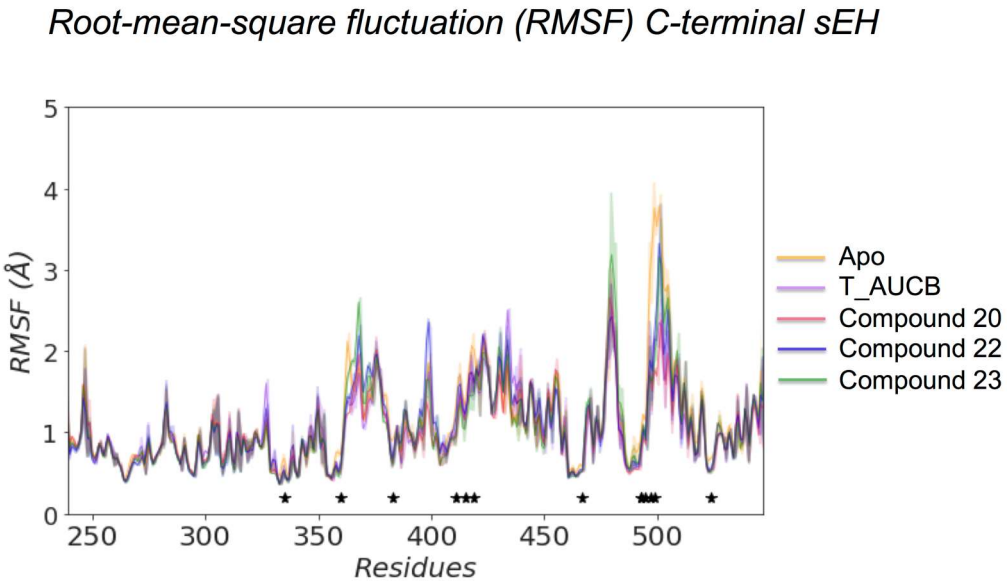


**Figure S2**: Root Mean Square Fluctuation (RMSF, in Å) of the C-terminal region of sEH either in the apo (orange line), *t*-AUCB bound (purple), compound **20** (red), **22** (blue), and **23** (green). Stars mark the sEH residues that occupy the active site region.

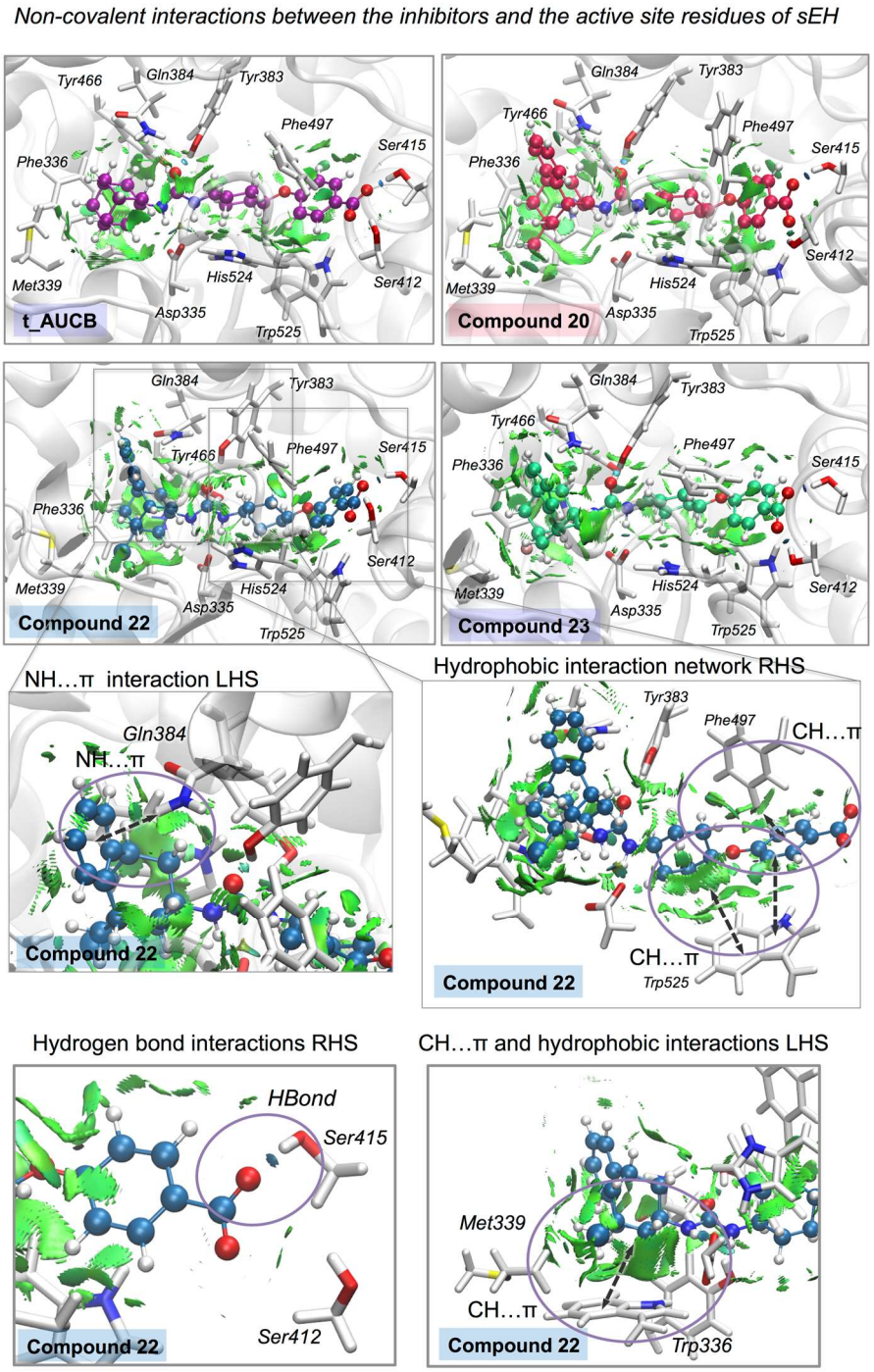


**Figure S3**: Representation of the noncovalent interactions (computed with NCIplot) at the active site of soluble epoxide hydrolase active site in the presence of compounds *t*-AUCB, **20**, **22**, and **23**. The weak interactions are shown as green surfaces, hydrogen-bonds are depicted in blue, and repulsive interactions in red. The interaction surface of the NH…π interation between the side chain of Gln384 and the aromatic ring of the benzohomoadamantane scaffold of compound **22** is highlighted. The network of hydrogen bonds, hydrophobic and CH…π interactions in both LHS and RHS pockets in the presence of compound **22** are depicted. The non-covalent interactions are calculated for the representative structures of the most populated cluster obtained from the MD simulations.

*Analysis of active site water molecules in MD simulations*

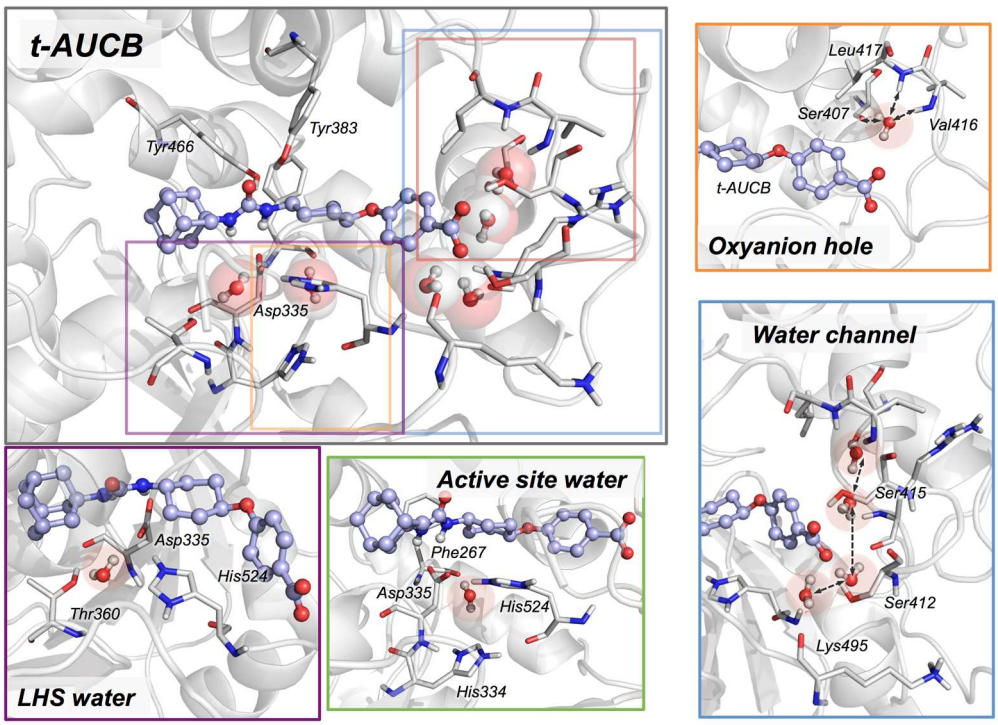


**Figure S4**: Representative MD snapshots displaying the water occupation in the RHS pocket in the presence of *t*-AUCB, oxyanion hole region, as well as the network of water channels are additionally provided. Representative MD snapshots showing the positioning of two water molecules: one occupying the RHS of the catalytic Asp335 (green panel), while the other one is positioned on the LHS (purple panel).

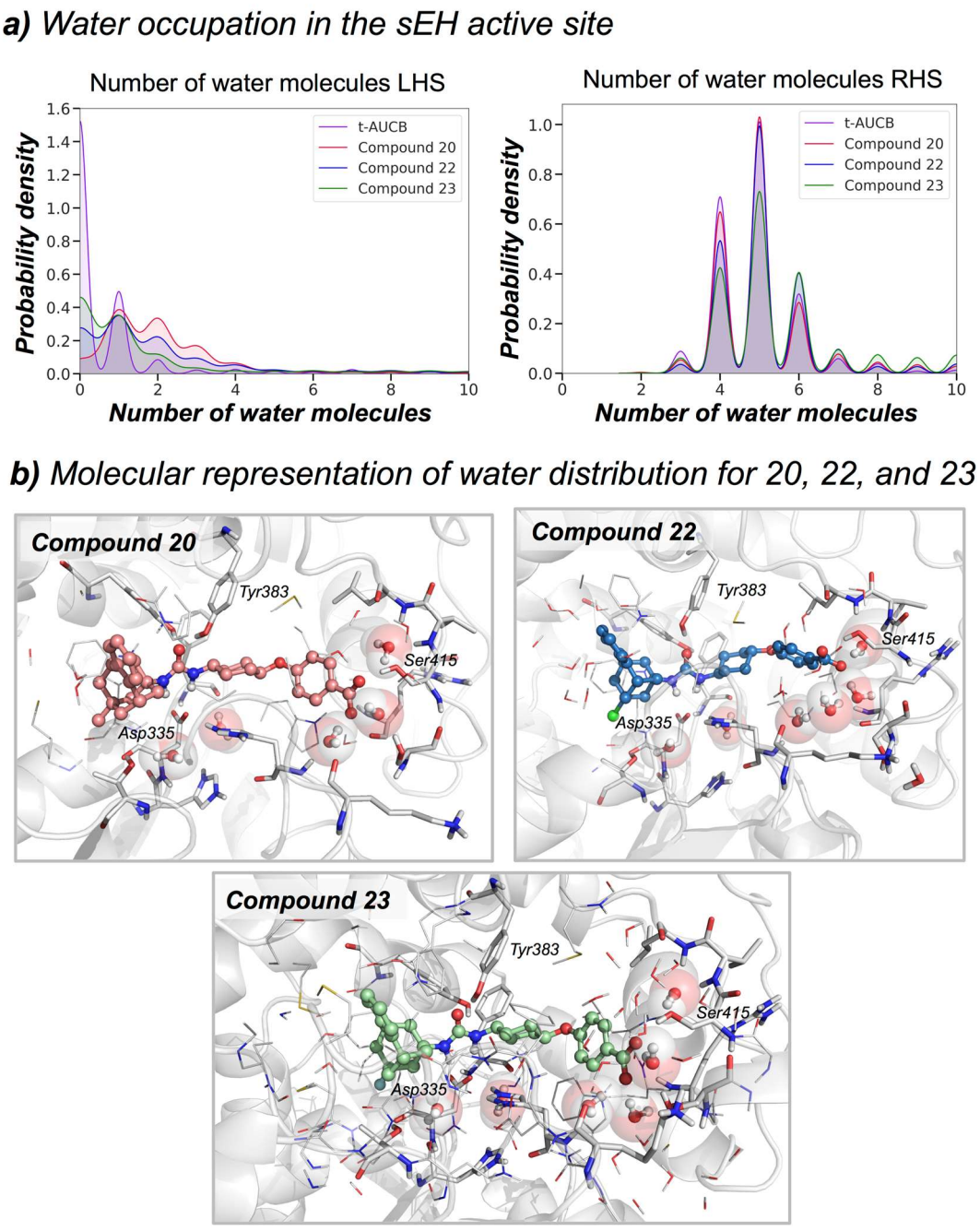


**Figure S5**: Representation of the normalized kernel density plot of the water distribution in the active site LHS and RHS pocket in the presence of *t*-AUCB (purple), **20** (red), **22** (blue), and **23** (green). We monitored the presence of water molecules through visual inspection of MD trajectories and using the *watershell* function of cpptraj MD analysis program.[2] Using *watershell*, we calculated the number of water molecules in the first solvation shell (using a distance cutoff of 3.4 Å) for both RHS (carboxylate group) and LHS (adamantane) pockets along the MD simulations. The average number of water molecules in the RHS pocket is 5.0 ± 1.4 (*t*-AUCB), 5.3 ± 1.8 (compound **20**), 5.6 ± 2.1 (compound **22**), and 6.1 ± 2.5 (compound **23**), respectively. The average number of water molecules in the LHS pocket is 1.0 ± 2.6 (*t*-AUCB), 2.8 ± 3.6 (compound **20**), 2.7 ± 3.9 (compound **22**), and 2.5 ± 4.5 (compound **23**).

***a)*** *Rotation of the (benzohomo)adamantane moiety in the left-hand-side pocket of the sEH active site along the MD simulations*

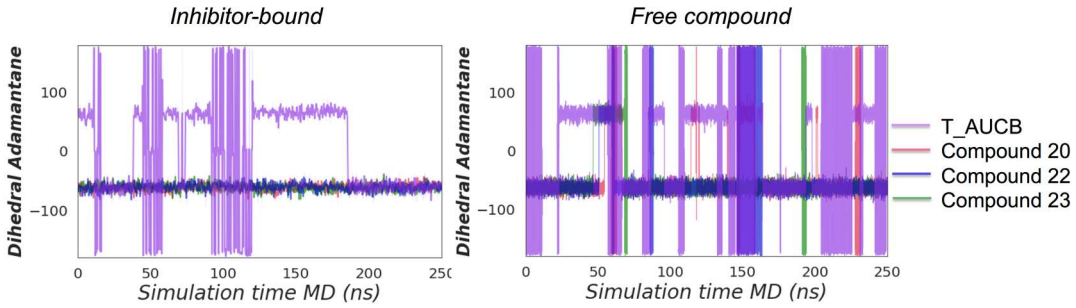


***b)*** *Representative dihedral angle that describes the rotation of the adamantane moiety*

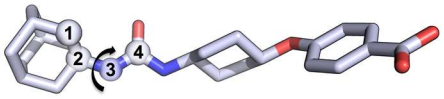


**Figure S6**: a) Plot of the dihedral angle that describes the rotation of the benzohomoadamantane moiety in the left-hand-side pocket of the sEH active site along the MD simulations (left) and when the compounds are free in the solvent (right). *t*-AUCB is shown in purple, compound **20** in red, compound **22** in blue, and compound **23** in green. b) Molecular representation of the dihedral angle used to monitor the rotation of the (benzohomo)adamantane scaffold.

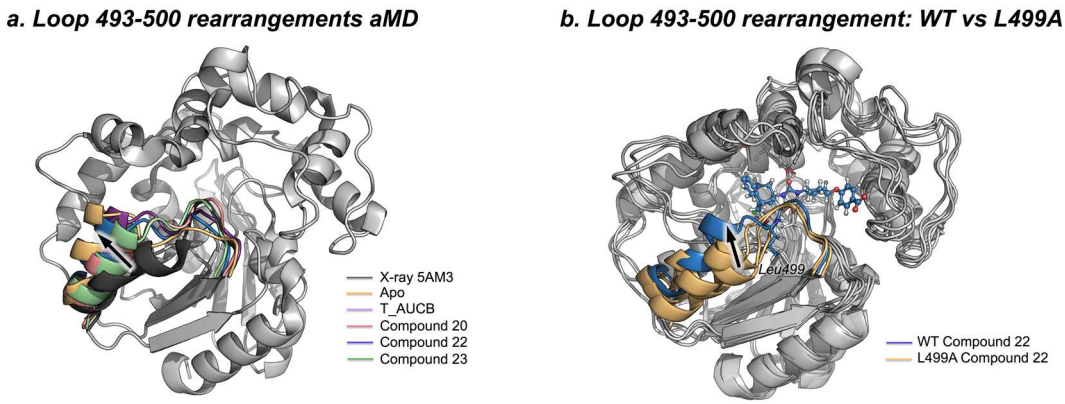


**Figure S7**: a) Overlay of the X-ray (in black), and representative snapshot from the apo state aMD simulations (yellow structure), and inhibitor-bound: *t*-AUCB (purple), and compounds **20** (red), **22** (blue), and **23** (green) simulations. The aMD parameters are calculated as described previously.[3] For *t*-AUCB, the boost potential applied to all dihedrals of the system is obtained from an energy threshold of 8101.08 kcal/mol and an alpha parameter value of 382.90 while a boost potential corresponding to an energy threshold of -217851.72 kcal/mol and alpha parameter of 12217.28 were applied to all atoms of the system. For **20**, the boost potential applied to all dihedrals of the system is obtained from an energy threshold of 8106.07 kcal/mol and an alpha parameter value of 382.90 while a boost potential corresponding to an energy threshold of -217635.12 kcal/mol and alpha parameter of 12218.88 were applied to all atoms of the system. For **22**, the boost potential applied to all dihedrals of the system is obtained from an energy threshold of 8101.1 kcal/mol and an alpha parameter value of 382.90 while a boost potential corresponding to an energy threshold of -217682.60 kcal/mol and alpha parameter of 12218.40 were applied to all atoms of the system. For **23**, the boost potential applied to all dihedrals of the system is obtained from an energy threshold of 8114.27 kcal/mol and an alpha parameter value of 382.90 while a boost potential corresponding to an energy threshold of -217735.60 kcal/mol and alpha parameter of 12218.40 were applied to all atoms of the system. B) Overlay of representative conventional MD snapshots for WT sEH (in blue), and three independent replicas of L499A variant (in yellow) showing the displacement of the loop 493-400 region.

| Time | ID | Total Concentration (ng/mL) | Mean (ng/mL) | SD (ng/mL) |
|---|---|---|---|---|
| 0 h | Mouse 1 | 0 | 0 | 0 |
| | Mouse2 | 0 | | |
| | Mouse3 | 0 | | |
| 0.25 h | Mouse 1 | 787 | 767.5 | 27.6 |
| | Mouse2 | 5400[a] | | |
| | Mouse3 | 748 | | |
| 0.5 h | Mouse 1 | 1470 | 1610.0 | 475.7 |
| | Mouse2 | 2140 | | |
| | Mouse3 | 1220 | | |
| 1 h | Mouse 1 | 1000 | 970.3 | 345.5 |
| | Mouse2 | 1300 | | |
| | Mouse3 | 611 | | |
| 2 h | Mouse 1 | 475 | 397.3 | 112.8 |
| | Mouse2 | 449 | | |
| | Mouse3 | 268 | | |
| 4 h | Mouse 1 | 0 | 51.9 | 45.4 |
| | Mouse2 | 71.3 | | |
| | Mouse3 | 84.3 | | |
| 6 h | Mouse 1 | 21.7 | 37.3 | 14.3 |
| | Mouse2 | 40.2 | | |
| | Mouse3 | 49.9 | | |
| 24 h | Mouse 1 | 0 | 0 | 0 |
| | Mouse2 | 0 | | |
| | Mouse3 | 0 | | |

**Table S2**: Mean of concentrations of **20** in mouse plasma at different times after ip administration at 3 mg/Kg. [a]This mouse was excluded for mean and SD calculations because it was considered as a significant outlier $P<0.05$.

| Time | ID | Total Concentration (ng/mL) | Mean (ng/mL) | SD (ng/mL) |
|---|---|---|---|---|
| 0 h | Mouse 1 | 0 | 0 | 0 |
| | Mouse2 | 0 | | |
| | Mouse3 | 0 | | |
| 0.25 h | Mouse 1 | 151 | 354.7 | 241.9 |
| | Mouse2 | 291 | | |
| | Mouse3 | 622 | | |
| 0.5 h | Mouse 1 | 1350 | 1616.7 | 325.9 |
| | Mouse2 | 1520 | | |
| | Mouse3 | 1980 | | |
| 1 h | Mouse 1 | 600 | 1446.7 | 1063.3 |
| | Mouse2 | 1100 | | |
| | Mouse3 | 2640 | | |
| 2 h | Mouse 1 | 2440.0 | 3583.3 | 1089.9 |
| | Mouse2 | 2640.0 | | |
| | Mouse3 | 5670.0 | | |
| 4 h | Mouse 1 | 1240.0 | 1516.7 | 387.9 |
| | Mouse2 | 1960.0 | | |
| | Mouse3 | 1350.0 | | |
| 6 h | Mouse 1 | 1160 | 1141.3 | 398.3 |
| | Mouse2 | 734.0 | | |
| | Mouse3 | 1530 | | |
| 24 h | Mouse 1 | 181.0 | 104.6 | 71.0 |
| | Mouse2 | 40.6 | | |
| | Mouse3 | 92.3 | | |

**Table S3**: Mean of concentrations of **22** in mouse plasma at different times after ip administration at 3 mg/kg.

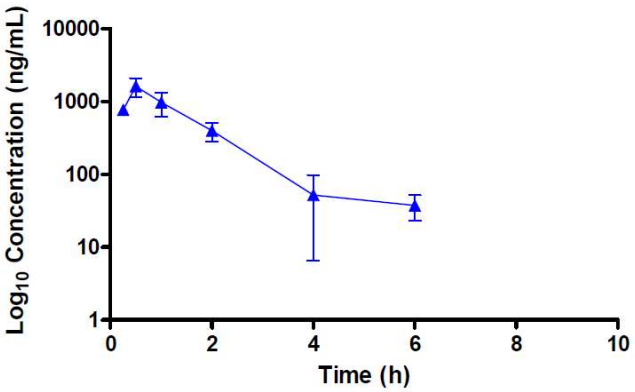


**Figure S8**: Plasma concentration (scale log 10) *vs* time for ip administration at 3 mg/kg of compound **20**.

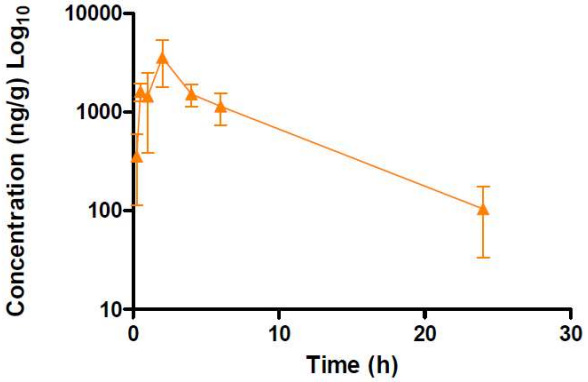


**Figure S9**: Plasma concentration (scale log 10) *vs* time for ip administration at 3 mg/kg of compound **22**.

| Control Group | Sample 1 | Sample 2 | Sample 3 | Sample 4 | Sample 5 |
|---|---|---|---|---|---|
| *Parenchymal atrophy* | 0 | 0 | 0 | 0 | 0 |
| *Vacuolar degeneration of cells* | 0 | 0 | 0 | 0 | 0 |
| *Edema* | 0 | 0 | 0 | 0 | 0 |
| *Hemorrhage* | 0 | 0 | 0 | 0 | 0 |
| *Mononuclear inflammatory cells* | 0 | 0 | 0 | 0 | 0 |
| *Polimorfonuclear inflammatory cells* | 0 | 0 | 0 | 0 | 0 |
| *Necrosis* | 0 | 0 | 0 | 0 | 0 |
| *Total* | 0 | 0 | 0 | 0 | 0 |

**Table S4**: Histologic scoring of pancreatic tissues of control group.

| Cerulein Group | Sample 1 | Sample 2 | Sample 3 | Sample 4 | Sample 5 |
|---|---|---|---|---|---|
| *Parenchymal atrophy* | 2 | 2 | 3 | 1 | 2 |
| *Vacuolar degeneration of cells* | 1 | 2 | 2 | 1 | 2 |
| *Edema* | 2 | 1 | 2 | 2 | 2 |
| *Hemorrhage* | 0 | 0 | 0 | 0 | 0 |
| *Mononuclear inflammatory cells* | 1 | 1 | 2 | 1 | 1 |
| *Polimorfonuclear inflammatory cells* | 1 | 2 | 3 | 1 | 2 |
| *Necrosis* | 1 | 0 | 2 | 1 | 0 |
| *Total* | 8 | 8 | 14 | 7 | 9 |

**Table S5**: Histologic scoring of pancreatic tissues of mice treated with cerulein.

| Cerulein + 22 (0.1 mg/Kg) | Sample 1 | Sample 2 | Sample 3 | Sample 4 | Sample 5 |
|---|---|---|---|---|---|
| *Parenchymal atrophy* | 3 | 1 | 0 | 1 | 3 |
| *Vacuolar degeneration of cells* | 1 | 0 | 0 | 0 | 2 |
| *Edema* | 2 | 3 | 0 | 1 | 2 |
| *Hemorrhage* | 0 | 0 | 0 | 0 | 0 |
| *Mononuclear inflammatory cells* | 1 | 0 | 0 | 0 | 0 |
| *Polimorfonuclear inflammatory cells* | 1 | 2 | 0 | 1 | 3 |
| *Necrosis* | 2 | 1 | 0 | 0 | 0 |
| *Total* | 10 | 7 | 0 | 3 | 11 |

**Table S6**: Histologic scoring of pancreatic tissues of mice treated with cerulein and **22** at 0.1 mg/kg.

| Cerulein + 22 (0.3 mg/Kg) | Sample 1 | Sample 2 | Sample 3 | Sample 4 | Sample 5 |
|---|---|---|---|---|---|
| *Parenchymal atrophy* | 1 | 0 | 1 | 1 | 2 |
| *Vacuolar degeneration of cells* | 0 | 0 | 1 | 0 | 1 |
| *Edema* | 1 | 1 | 1 | 1 | 0 |
| *Hemorrhage* | 0 | 0 | 0 | 0 | 0 |
| *Mononuclear inflammatory cells* | 0 | 0 | 0 | 0 | 0 |
| *Polimorfonuclear inflammatory cells* | 1 | 0 | 1 | 1 | 1 |
| *Necrosis* | 0 | 0 | 0 | 0 | 0 |
| *Total* | 3 | 1 | 4 | 3 | 4 |

**Table S7**: Histologic scoring of pancreatic tissues of mice treated with cerulein and **22** at 0.3 mg/kg.

## REFERENCES


1- Durrant, J. D.; Votapka, L.; Sorensen, J.; Amaro, R. E. POVME 2.0: An enhanced tool for determining pocket shape and volume characteristics. *J. Chem. Theory Comput.* **2014**, *10*, 5047–5056.

2- Roe, D. R.; Cheatham, T. E., III. PTRAJ and CPPTRAJ: Software for processing and analysis of molecular dynamics trajectory data. *J. Chem. Theory Comput.* **2013**, *9*, 3084–3095.

3- Hamelberg, D.; de Oliveira, C. A. F.; McCammon, J. A. Sampling of slow diffusive conformational transitions with accelerated molecular dynamics. *J. Chem. Phys.* **2007**, *127*, 155102.